Molecular Biology of the Cell
Vol. 18, 3081–3093, August 2007

Naked2 Acts as a Cargo Recognition and Targeting Protein to Ensure Proper Delivery and Fusion of TGF-α–containing Exocytic Vesicles at the Lower Lateral Membrane of Polarized MDCK Cells[D] [V]

Cunxi Li,* Mingming Hao,† Zheng Cao,* Wei Ding,* Ramona Graves-Deal,* Jianyong Hu,* David W. Piston,† and Robert J. Coffey*‡

Departments of *Medicine and Cell and Developmental Biology and †Molecular Physiology and Biophysics, Vanderbilt University Medical Center, Nashville, TN 37232; and ‡Department of Veterans Affairs Medical Center, Nashville, TN 37232-2279

Submitted February 26, 2007; Revised May 18, 2007; Accepted May 24, 2007
Monitoring Editor: Jennifer Lippincott-Schwartz

Transforming growth factor-α (TGF-α) is the major autocrine EGF receptor ligand in vivo. In polarized epithelial cells, proTGF-α is synthesized and then delivered to the basolateral cell surface. We previously reported that Naked2 interacts with basolateral sorting determinants in the cytoplasmic tail of a Golgi-processed form of TGF-α and that TGF-α is not detected at the basolateral surface of Madin-Darby canine kidney (MDCK) cells expressing myristoylation-deficient (G2A) Naked2. By high-resolution microscopy, we now show that wild-type, but not G2A, Naked2-associated vesicles fuse at the plasma membrane. We further demonstrate that Naked2-associated vesicles are delivered to the lower lateral membrane of polarized MDCK cells independent of μ1B adaptin. We identify a basolateral targeting segment within Naked2; residues 1-173 redirect NHERF-1 from the apical cytoplasm to the basolateral membrane, and internal deletion of residues 37-104 results in apical mislocalization of Naked2 and TGF-α. Short hairpin RNA knockdown of Naked2 leads to a dramatic reduction in the 16-kDa cell surface isoform of TGF-α and increased cytosolic TGF-α immunoreactivity. We propose that Naked2 acts as a cargo recognition and targeting (CaRT) protein to ensure proper delivery, tethering, and fusion of TGF-α–containing vesicles to a distinct region at the basolateral surface of polarized epithelial cells.

INTRODUCTION

All seven mammalian EGF receptor (EGFR) ligands (EGF, TGF-α [TGFα], amphiregulin, heparin-binding EGF-like growth factor, betacellulin, epiregulin and epigen) are type 1 transmembrane proteins that are produced by many epithelial cell types (Harris *et al.*, 2003). The fidelity of trafficking of these endogenous EGFR ligands to the proper cell surface in normal polarized epithelial cells is highly relevant since the EGFR is restricted to the basolateral membrane. TGFα is delivered preferentially to the basolateral cell surface of polarized epithelial cells where it is rapidly cleaved by TNF-α converting enzyme/a disintegrin and metalloprotease (TACE/ADAM-17; Dempsey and Coffey, 1994; Sunnarborg *et al.*, 2002). Soluble TGFα is then avidly captured by basolateral EGFRs (Dempsey and Coffey, 1994). The rapid cleavage and avid capture of this ligand suggest that cell surface delivery may be a critical, and possibly rate-limiting, step in the posttranslational regulation of endogenous TGFα activity.

Basolateral sorting information usually resides in the cytoplasmic tail of basolaterally targeted cargo. TGFα's cytoplasmic tail, the most highly conserved portion of the molecule across species, contains domains that affect its trafficking through the secretory pathway. The C-terminus contains a type 1 PDZ recognition domain (ETVV). The PDZ-containing proteins syntenin (Fernandez-Larrea *et al.*, 1999), GRASP55 (Kuo *et al.*, 2000), and membrane-associated guanylate kinase inverted (MAGI)-2 and -3 (Franklin *et al.*, 2005) bind this motif early in the secretory pathway. This domain contributes to the efficiency, but not the fidelity, of trafficking because TGFα is still delivered preferentially, albeit less efficiently, to the basolateral surface of polarized epithelial cells in the absence of ETVV (Franklin *et al.*, 2005).

Two basolateral-sorting determinants in the cytoplasmic tail of TGFα have been identified (LL and HCCQVRKH; Dempsey *et al.*, 2003). We recently reported that Naked2 binds to these domains but not to TGFα's PDZ recognition domain (Li *et al.*, 2004). Naked1 and 2 are the two mammalian orthologues of Naked Cuticle, an inducible negative regulator of canonical Wnt signaling as determined by genetic analysis in *Drosophila* (Rousset *et al.*, 2001; Yan *et al.*,

This article was published online ahead of print in *MBC in Press* (http://www.molbiolcell.org/cgi/doi/10.1091/mbc.E07–02–0172) on June 6, 2007.

[D] [V] The online version of this article contains supplemental material at *MBC Online* (http://www.molbiolcell.org).

Address correspondence to: Robert J. Coffey (robert.coffey@vanderbilt.edu).

Abbreviations used: TGFα, transforming growth factor-α; HA, hemagglutinin epitope tag; MDCK, Madin-Darby canine kidney; LLC-PK1, Lilly Laboratories, Culture-Pig Kidney type1; EGF, epidermal growth factor; PDZ, PSD-95/SAP90, Discs large and Zona Occludens-1; G2A, 2nd residue glycine replaced by alanine; TGN, *trans*-Golgi network; LDLR, low-density lipoprotein receptor; VSV-G, vesicular stomatitis virus-glycoprotein.

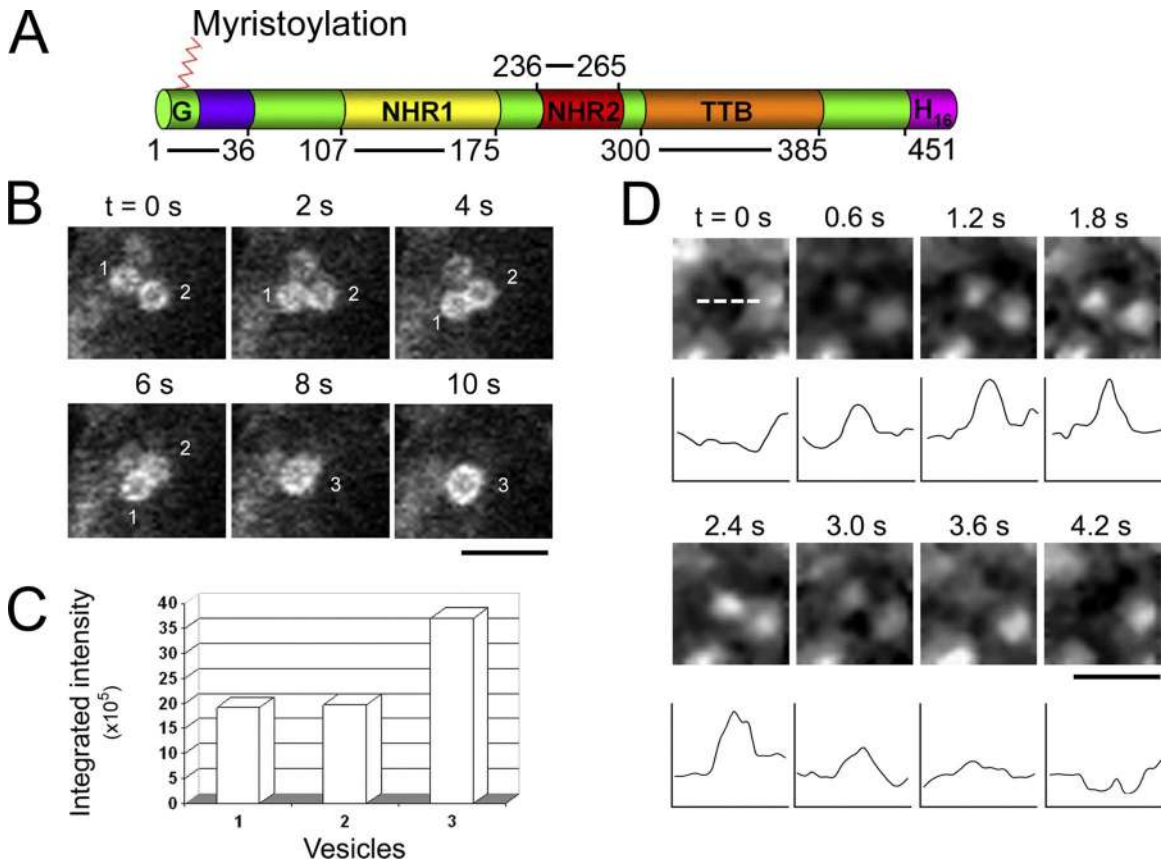

Figure 1. Naked2-associated vesicle fusion events. (A) Domains of human Naked2. Glycine, the second residue, undergoes myristoylation. Naked homologue region 1 (NHR1) consists of residues 107-175; NHR2 includes residues 236-265; TGFα tail-binding domain (TTB) was mapped to residues 300-385 (Li *et al.*, 2004), and H16 represents the last 22 residues that contain 16 histidines. (B) Live cell microscopy of a typical homotypic vesicle–vesicle fusion event. Bar, 1 μm. (C) For vesicles 1, 2, and 3, the integrated intensities (area X gray scale) were quantified by Metamorph software. (D) Time-lapse images were captured by total internal reflection fluorescent microscopy (TIR-FM) to visualize vesicle fusion at the plasma membrane. MDCK cells stably transfected with wild-type Naked2-EGFP were seeded onto MatTek dishes for 24 h, and then TIR-FM was performed. The microscope stage was maintained at 34°C. Scanning time was 200 ms for each 512 × 512 pixel image at 500-ms intervals. The dashed line indicates a region where a vesicle fusion event occurs. Quantification of fluorescent intensity is shown under each selected region. Bars, 2 μm.

2001). Naked Cuticle appears to act by binding and inactivating Dishevelled, a positive regulator of Wnt signaling. There are four regions conserved between Naked1 and Naked2 (Figure 1A). The most conserved region among Naked family members is Naked homologous region 1 (NHR1), residues 107-175 in human Naked2, which contains an EF-hand motif. For Naked1, this motif binds Dishevelled and Zn^{2+}, but not Ca^{2+}; Naked2's affinity to Dishevelled is weaker (Rousset *et al.*, 2002; Wharton, 2003). Mice with a targeted deletion of the EF-hand region of Naked1 exhibit reduced spermatogenesis but otherwise appear normal (Li *et al.*, 2005). The remaining three conserved regions between Naked1 and 2 are as follows: 1) the N-terminal 36 amino acids that include glycine as the second residue that is myristoylated along with adjacent *cis*-acting basic residues; 2) residues 236-265 in human Naked2 (Naked homologous region 2 [NHR2]); and 3) a C-terminal polyhistidine stretch. Naked2, but not Naked1, recognizes a Golgi-processed form of TGFα and binds TGFα between residues 300-385 (TGFα cytoplasmic tail-binding domain [TTB]), a sequence in Naked2 that diverges from Naked1. Naked2 coats TGFα-containing exocytic vesicles after the *trans*-Golgi network (TGN) and escorts these vesicles to the plasma membrane. In myristoylation-deficient G2A Naked2-expressing Madin-Darby canine kidney (MDCK) cells, Naked2 vesicles accumulate at a basolateral corner of the cell, and TGFα is unable to reach the plasma membrane. These effects appear to be specific for TGFα because amphiregulin, another basolaterally targeted EGFR ligand, is found at the cell surface of both wild-type and myristoylation-deficient G2A Naked2-expressing MDCK cells (Li *et al.*, 2004).

The present studies were designed to determine how Naked2 delivers these TGFα-containing vesicles to their proper destination. We addressed whether Naked2 utilizes a Sec6/8 exocyst complex beneath the tight junctions for basolateral docking and fusion as has been reported for low-density lipoprotein receptor (LDLR) and VSV-G (Kreitzer *et al.*, 2003; Polishchuk *et al.*, 2004) and whether the μ1B subunit of the epithelial cell–specific AP-1B adaptor complex is required for basolateral trafficking of Naked2 and TGFα as it is for the LDLR (Folsch *et al.*, 1999). Herein we show that myristoylation of Naked2 is required for these vesicles to fuse at the plasma membrane. We provide evidence that discrete residues within the N-terminus of Naked2 direct these vesicles to the basolateral cell surface. Residues 1-173 redirect Na^+/H^+ exchanger regulatory factor (NHERF)-1 from the apical cytoplasm to the basolateral membrane and internal deletion of residues 37-104 results in apical mislocalization

of Naked2 and TGFα. Naked2-associated vesicles are directed to the lower lateral membrane of polarized MDCK cells and do not appear to require μ1B nor utilize the subapical Sec6/8 exocyst complex as a targeting patch for basolateral docking and fusion. We propose that Naked2 acts as a cargo recognition and targeting (CaRT) protein to ensure proper targeting, tethering and fusion of TGFα-containing exocytic vesicles at the lower lateral membrane of polarized MDCK cells.

MATERIALS AND METHODS

Reagents, Cell Lines, and cDNA

All cell culture reagents were from Hyclone (Logan, UT). All chemicals, mAb 100.3 anti-γ adaptin, mouse anti-hemagglutinin (HA), anti-Flag, and anti-clathrin antibodies were from Sigma Chemical Co. (St. Louis, MO) unless otherwise stated. Anti-β1/2 adaptins (10A) was generously provided by T. Kirchhausen (Harvard Medical School). RY/1, mouse anti-μ1 antibody, was kindly provided by L. Traub (University of Pittsburgh School of Medicine), and anti-μ1B polyclonal antibody was a gift from I. Mellman (Yale University School of Medicine). Rabbit anti-DVL1 antibody was generously provided by A. Wynshaw-Boris (University of California, San Diego). Rabbit anti-MPR300 and anti-μ4 antibodies were from S. Hoening (Georg-August University, Göttingen, Germany). Polyclonal sheep anti-human TGFα serum was made in collaboration with East Acres Biologicals (Southbridge, MA). Antibodies against GM130, TGN38, Golgin97, Rab8, Rab11A, and Rab11B were provided by James R. Goldenring (Vanderbilt University). Rabbit anti-ZO1 antibody was purchased from Zymed Laboratories (San Francisco, CA). Rhodamine-phalloidin, Alexa 594–conjugated goat anti-mouse IgG, Alexa 488-conjugated anti-rabbit IgG and Alexa 488–conjugated donkey anti-goat IgG were from Molecular Probes (Eugene, OR). Mouse anti-Sec6 antibody was purchased from CALBIOCHEM (Darmstadt, Germany). mAb of MTCO2 (ab3298-500) was obtained from Abcam (Cambridge, MA). Rabbit anti-DsRed2 antibody was from Clontech (Palo Alto, CA). Goat anti-α adaptin antibody was from Santa Cruz Biotechnology (Santa Cruz, CA). Cy3-conjugated donkey anti-sheep IgG and horseradish peroxidase (HRP)-conjugated donkey anti-mouse IgG were from Jackson ImmunoResearch Laboratories (West Grove, PA). The TACE/ADAM17 inhibitor WAY-022 was provided by Jay Gibbons (Wyeth Ayerst, Pearl River, NY). All electrophoresis reagents were purchased from Bio-Rad Laboratories (Belmont, CA).

LLC-PK_1 cells, HEK 293 cells, MDCK Tet-Off cells T23 1628 (Clontech), and all stably transfected cells were grown in Dulbecco's modified Eagle's medium (DMEM) supplemented with 10% fetal bovine serum (FBS), glutamine, nonessential amino acids, 100 U/ml penicillin, 100 μg/ml streptomycin, and with or without 500 μg/ml geneticin and or 200 μg/ml hygromycin (Roche, Mannheim, Germany). Doxycycline (1 μg/ml) was used to regulate expression of Naked2 mutants. For experiments on Transwell filters, 1×10^5 cells were seeded on 12-mm Transwell filter chambers (0.4 μm, Costar, Corning, Corning, NY) and cultured for 3-4 d with replenishment of medium every other day unless otherwise stated. To assess the integrity of tight junctions, transepithelial electrical resistance was measured using the Millicell Electrical Resistance system (Millipore, Bedford, MA). All experiments with polarized cells were performed when electrical resistance of MDCK cells was >200 Ω/cm^2.

Plasmids and Transfection

Full-length human Naked2 was obtained by PCR amplification of human RACE-ready cDNA (Li *et al.*, 2004). All 5′ primers contained an EcoRI or NheI restriction endonuclease site, and all 3′ primers contained a BamHI or SacI site. Internal deletion sites were introduced using a SacI restriction endonuclease site by PCR. cDNA of human NHERF-1 was cloned from HCA-7 cells by RT-PCR with introduction of SacI and BamHI sites at the 5′ and 3′ ends, respectively. All PCR-generated constructs were verified by automated DNA sequencing (Perkin Elmer-Cetus 377, Vanderbilt Ingram Cancer Center DNA Sequencing Shared Resource). pDsRed2-Mito, pEGFP-N2, and pDsRed2-N1 were purchased from Clontech. Reagents and their generous providers are as follows: canine Rab7a cDNA, mCherry-hRab5a, myosin Va, b, and c (James R. Goldenring); pEGFP-LDLR, pCB6-μ1B-HA and anti-μ1B antibody (I. Mellman); HA and Flag dual-tagged proTGFα (David Lee, University of North Carolina; Briley *et al.*, 1997); pmCherry-clathrin light chain plasmid (J. H. Keen, Thomas Jefferson University); a retroviral p120-EGFP (Albert Reynolds, Vanderbilt University). pDsRed2-μ2 was cloned from pACT2-μ2. All primers were synthesized by Invitrogen (Carlsbad, CA). BglII and SacI were introduced into the 5′ and 3′ primers, respectively.

Stable transfections of MDCK cells were performed using FuGENE 6 (Roche) according to the manufacturer's instructions. Clonal cell lines stably expressing wild-type human proTGFα cDNA in vector pCB7 were maintained in DMEM medium containing 200 μg/ml hygromycin. MDCK cells that were incubated for 24 or 48 h after transient transfection with blank vectors and the chimeras were fixed in 4% paraformaldehyde for 30 min. Transfection of Naked2 deletion mutants and Naked2 chimeras fused to pEGFP-N2 and pDsRed2-N1 were selected in DMEM medium containing 500 μg/ml geneticin. Tet-off cells were maintained with or without 1 μg/ml doxycycline. At least three individual clones were isolated for each stably transfected cell line.

Tannic Acid Blocking

Polarized MDCK cells stably transfected with Naked2-EGFP or p120-EGFP were heat-bleached at 40°C for 4-6 h. Precooled medium with or without 0.5% tannic acid was applied immediately either apically or basolaterally until the plates were put into a 10°C incubator for 20 min. Then the plates were moved into a 37°C incubator for 0, 15, 30, 60, and 120 min. After 4% paraformaldehyde fixation, F-actin was stained with rhodamine-phalloidin (red) to outline the cell borders. Mean fluorescent intensity and SD were calculated from at least three separate experiments.

Yeast Two- and Three-Hybrid Assays

Two-hybrid analysis between various Naked2 fragments and the adaptor subunits was carried out in AH109 yeast cells. The adaptor subunits constructed in AD vectors were generously provided by Juan Bonifacino (National Institutes of Health) (Janvier *et al.*, 2003). Naked2 N-terminal fragments were constructed in DNA-BD vector pGBKT7. Transformation was performed by the lithium acetate procedure as described in the instruction for the MATCHMAKER two-hybrid kit (Clontech). AH109 transformants were selected and maintained on plates lacking leucine and tryptophan. For colony growth assays, AH109 transformants were dotted on plates lacking leucine, tryptophan, and histidine and allowed to grow at 30°C with 5 mM 3-amino-1, 2,4-triazole for 5 d.

Light Microscopy and Live Cell Microscopy

MDCK cells cultured on plastic were fixed with 4% paraformaldehyde for 15 min. Cells cultured on 12-mm Transwell filters (Costar) were washed twice with cold phosphate-buffered saline (PBS), fixed with 4% paraformaldehyde for 30 min, permeabilized with 0.5% Triton X-100 for 10 min, blocked for 1 h in 2% BSA, and incubated subsequently with primary antibodies and Alexa 594– or Alexa 488–labeled secondary antibodies. Immunofluorescence was visualized using a Zeiss LSM 510 confocal microscope and a Zeiss Axiophot microscope (Thornwood, NY; Vanderbilt Ingram Cancer Center Cell Imaging Shared Resource). All micrographs were taken using 40× objective lens.

For time-lapse confocal microscopy, a specific focal plane was taken to examine the movement of the enhanced green fluorescent protein (EGFP)-tagged Naked2 vesicles and possible fusion events between vesicle–vesicle and vesicle–plasma membrane on MatTek plates. Time-lapse images were taken at 2-s intervals for 5 min using the Zeiss LSM 510. Cells were kept at 37°C and 5% CO_2 with a controlled stage (Bioptechs, Butler, PA; Delta T System). The integrated intensity of the captured images was measured by using MetaMorph imaging software (Universal Imaging, West Chester, PA). To investigate the vesicle trafficking in polarized epithelial cells, MDCK cells stably transfected with Naked2-EGFP were polarized on the undersurface of the Transwell filters for 4-5 d when electrical resistance exceeded 200 Ω/cm^2. The inserts were transferred into MatTek dishes (Ashland, MA) with phenol red–free medium and maintained in a 37°C and 5% CO_2 chamber for live cell microscopy. Time-lapse images were taken from six sequential planes from the midpoint to the base of the cell at 2.5-s intervals. The relative fluorescent intensity of the selected vesicles was manually traced, tracked, and quantified in six focal planes through 20 time points.

Cell surface immunofluorescent staining of HA-TGFα was performed on fully polarized, live MDCK cells that had been transfected with pcDNA3.1-HA-TGFα and pEGFPN2-Naked2Δ37-104. Cells were treated with the TACE inhibitor, WAY-022 (1 μm), for 1 h and then placed on ice for 10 min. Anti-HA mAb was diluted in DMEM with 10% fetal calf serum and incubated apically and basolaterally for 1 h at 4°C. After washing three times with cold PBS, MDCK cells were fixed with 4% paraformaldehyde and then stained with Cy3-donkey anti-mouse antibody.

Total Internal Reflection Fluorescence Microscopy

MDCK cells stably transfected with wild-type Naked2 and G2A mutant Naked2 were seeded on MatTek plates for 24 h. Total internal reflection fluorescence microscopy (TIR-FM) images were obtained with an Olympus IX-70 using a TIR-FM illumination system (Olympus, Melville, NY) and a dual-view multi-image acquisition system (Optical Insights, Santa Fe, NM) equipped with an Orca ER camera (Hamamatsu, Bridgewater, NJ) and supported by the Wasabi software package (Hamamatsu). Each set of TIR-FM images was taken with a 300-ms exposure for 3 min. Temperature of the microscope stage was maintained at 34°C. Images were analyzed using MetaMorph imaging software (Universal Imaging).

Biochemical Fractionation

We have adapted the protocol from OptiPrep (Axis Shiels, Oslo, Norway). For vesicle purification, MDCK cells stably transfected with EGFP-tagged Naked2

cDNA were grown to near confluence on plastic. At the time of harvest, the cells were rinsed three times in 1× PBS and then washed once in ice-cold solution D (50 mm HEPES, 78 mm KCl, 4 mm $MgCl_2$, 8.4 mm $CaCl_2$, 10 mm EGTA, pH 7.0). Ice-cold solution E (8.5 g sucrose dissolved in 100 ml solution D) was added, and cells were scraped off with a rubber policeman. Lysates were homogenized for 30 min on ice using a 30-ml Dounce homogenizer and a Potter homogenizer (Wheaton Scientific Products, Mellville, NJ). Successive centrifugations were performed on the supernatants at 1000 × *g* (10 min), 5000 × *g* (10 min), 10,000 × *g* (20 min), and 15,000 × *g* (20 min) using a fixed-angle SA600 rotor and at 100,000 × *g* (1 h) using a SW28 swinging-bucket rotor. The final vesicle-enriched pellet was designated as the crude vesicle fraction. It was resuspended in 2 ml of solution E, and one milliliter was placed on the top of duplicate 10–40% Iodixanol gradients (12 ml volume). These gradients were centrifuged at 90,000 × *g* for 18 h in a TH641 swinging-bucket rotor. Gradient fractions were collected in 0.5-ml aliquots, and optical densities were read at 260 and 280. An aliquot from each fraction was used for Western blotting and for TGFα radioimmunoassay (RIA). Blots were probed with R44 and various membrane and organelle markers.

Naked2 Knockdown

One set of short hairpin RNA (shRNA) constructs against human Naked2 mediated by pRS, a retroviral carrier, was purchased from OriGene (TR302950, Rockville, MD). The region TGCCAGTGATCCAGCGGCAC-GAGCACCAC was an efficient target sequence. Infectious virus was packaged in Phoenix cells. HaCat23 cells were infected twice with Phoenix cell supernatants that were filtered with Steriflip (Millipore, Billerica, MA), and pools were selected upon addition of 1 μg/ml puromycin.

RESULTS

Behavior of Naked2-associated Vesicles by Live Cell Microscopy and TIR-FM

The conserved regions and functional domains of Naked2 are depicted in Figure 1A. To observe the dynamic behavior of Naked2-associated vesicles, MDCK cells stably overexpressing wild-type Naked2-EGFP were cultured on MatTek glass bottom microwells and examined by live cell microscopy. Vesicles appeared to move to one corner of the cell. The fluorescent intensity of individual vesicles diminished over time and then disappeared. In the Supplementary Video 1 in Supplementary Material, the arrows point to representative fluorescent vesicles that appear to attach to the plasma membrane followed by diminution and loss of fluorescence. Some wild-type Naked2 vesicles "kiss and run," whereas others "touch and fuse." An example of a homotypic Naked2-associated vesicle–vesicle fusion event is shown in Figure 1B; a typical Naked2 vesicle–vesicle fusion event was completed in <8 s. The integrated intensity of a fused vesicle compared with the two parent vesicles was quantified in Figure 1C. We did not observe Naked2-associated tubular transport intermediates (Hirschberg *et al.*, 1998). The speed of vesicle movement was variable; there was an association between vesicle size and speed with the smallest vesicles (0.5 mm) tending to move the fastest (0.3 mm/s; data not shown).

To confirm that attachment of wild-type Naked2-associated vesicles at the cell surface represents fusion of vesicles at the plasma membrane, TIR-FM was performed using wild-type Naked2-EGFP–expressing MDCK cells cultured as described above (Figure 1D). Sequential frames from a representative TIR-FM image set are shown as an example of vesicle fusion at the plasma membrane. Each set of TIR-FM images was taken every 300 ms for 3 min. The selected region where fluorescent intensity was measured (indicated by the dashed line) showed an increase in intensity as the vesicle moved toward the plasma membrane. The peak of intensity (corresponding to the vesicle docking time) lasted 1.8 s and then decreased in intensity as fluorescence dissipated into the surrounding area over 4 s. The time course of fusion is similar to that for VSV-G–containing vesicles (Hirschberg *et al.*, 1998). This process was quantified over time in the linescan intensity profile of the vesicle under each image. These results provide unequivocal evidence that wild-type Naked2-associated vesicles fuse at the plasma membrane.

The behavior of myristoylation-deficient G2A Naked2-EGFP–associated vesicles differed dramatically. By live cell microscopy, these vesicles were more homogeneous in size, slower moving and separate, i.e., they did not interact with each other, nor did they appear to attach to the plasma membrane. Moreover, no membrane fusion events were detected by TIR-FM, although some EGFP-tagged myristoylation-deficient (G2A) Naked2 vesicles moved near the plasma membrane (data not shown). Thus, myristoylation of Naked2 appears to be required for both vesicle–vesicle and vesicle–plasma membrane fusion.

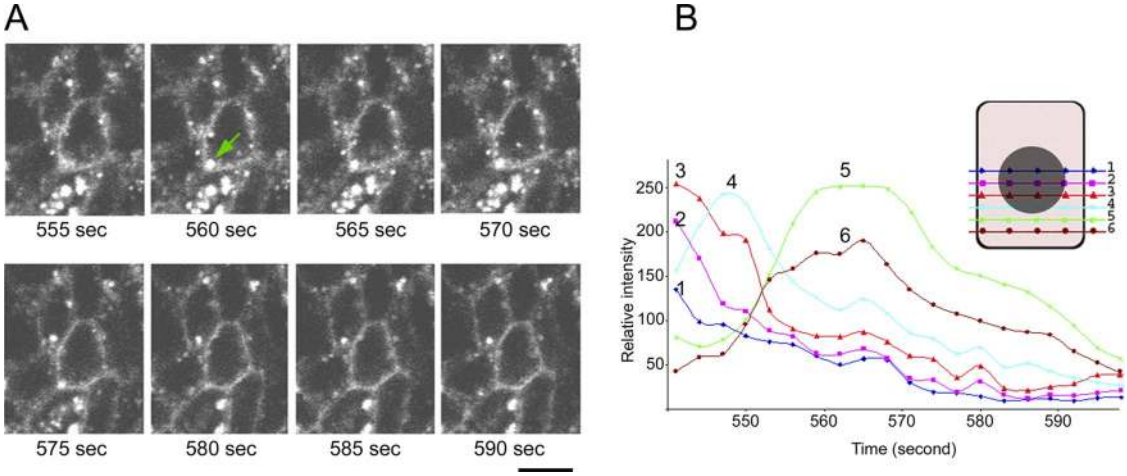

Figure 2. Live cell microscopy of Naked2-associated vesicles in polarized MDCK cells. (A) MDCK cells stably transfected with Naked2-EGFP were plated on the undersurface of Transwell filters, and experiments were performed on day 4 when electrical resistance exceeded 200 Ω/cm². Time-lapse images were taken from six sequential planes from the midpoint to the base of the cell at 2.5-s intervals as indicated in the top right corner of B. The green arrow in A indicates a representative vesicle visualized at the 5th plane. Fluorescent intensity of the vesicle diminishes over time in this plane. (B) The relative fluorescent intensity of the selected vesicle in A was manually traced, tracked, and quantified in six *Z*-sections at 20 time points over the last 60 s of the time-lapse movie. Bar, 10 μm.

Naked2-associated Vesicles Are Delivered to the Lower Portion of the Basolateral Plasma Membrane

LDLR and VSV-G both target directly to a Sec6/8 exocyst complex just below tight junctions (Kreitzer *et al.*, 2003; Polishchuk *et al.*, 2004). We previously observed that myristoylation-deficient G2A Naked2-associated vesicles accumulate asymmetrically at the basolateral corner of polarized MDCK cells (Li *et al.*, 2004). To observe the site of docking and fusion of wild-type Naked2-associated vesicles in polarized MDCK cells, we used live cell microscopy. MDCK cells were plated onto the undersurface of Transwell filters and maintained for 4 d at which time electrical resistance exceeded 200 Ω/cm^2. Transwell inserts were placed into MatTek glass-bottom microwells with medium, and the behavior of Naked2-associated vesicles was observed by confocal microscopy. Naked2-associated vesicles were observed throughout the cytoplasm. Vesicle membrane docking and fusion events were observed by 1-μm thickness scans captured every 2.5 s for 10 min. By selecting the midpoint of the *Z*-axis as the first focal plane and scanning to the base of the cell, we studied six optical sections covering roughly 6 μm in the *Z*-axis. Figure 2A shows one representative vesicle at focal plane 5 (indicated by the arrow). The vesicle first appeared in focal plane 2 and became more obvious in focal plane 3 before moving down to focal plane 5. The vesicle then moved toward the corner of the cell and disappeared at the membrane boundary of three adjacent cells. To assure ourselves that the disappearance of the vesicle was due to fusion with the plasma membrane and not movement to a different focal plane, the intensity of this vesicle was quantified in different *Z*-sections during a 10-min time course. The selected vesicle was manually traced and tracked in six *Z*-sections at 20 time points toward the end of a 10-min time-lapse movie. For each time point, the position of the vesicle was determined in the plane in which it was the brightest, and the integrated intensity of that position was measured in all six planes. From 560 s to the end of the movie, the intensity of this vesicle did not increase in any other focal plane (Figure 2B).

Studies were then undertaken to more precisely determine the initial site of docking and fusion of Naked2-associated vesicles along the basolateral compartment of polarized MDCK cells. We observed a loss of GFP fluorescence when stably transfected Naked2-EGFP–expressing MDCK

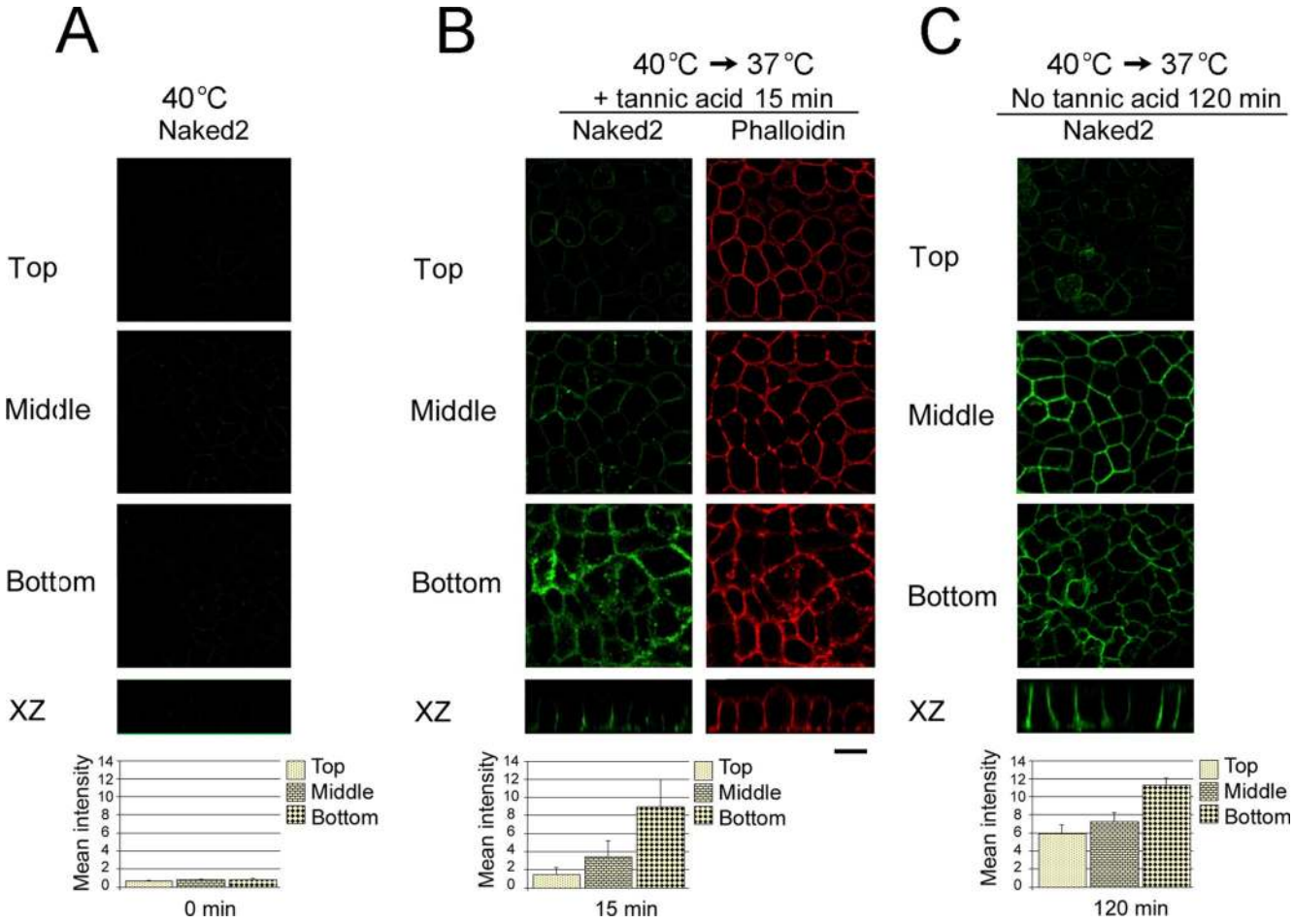

Figure 3. Tannic acid prevents cell surface fusion of Naked2-associated vesicles at the lower portion of the lateral plasma membrane of polarized MDCK cells. (A) MDCK cells stably transfected with Naked2-EGFP cDNA were cultured on Transwell filters for 4 d and then placed at 40°C for 4 h; this "heat bleaching" resulted in disappearance of GFP fluorescence. (B) After this 40°C heat bleaching, cells were then placed at 10°C for 10 min with 0.5% tannic acid added selectively to the basolateral medium, and then cells were restored to 37°C for 15 min in the continued presence of tannic acid. At this time, Naked2 fluorescence appeared at the lower lateral corner. (C) When cells were restored to 37°C for 2 h after 40°C heat bleaching in the absence of tannic acid, Naked2 fluorescence was found along the entire lateral membrane. F-actin was stained with rhodamine-phalloidin (red) to outline the cell borders. Mean fluorescent intensity ± SD from at least three separate experiments is shown under the representative image. Bar, 10 μm.

cells were maintained for 4 d on Transwell filters under standard 37°C culture conditions and then placed at 40°C for 4 h (Figure 3A); Western blotting and immunohistochemical staining with our Naked2 antibody R44 showed that Naked2 protein was present at this time but staining was diffuse in the cytoplasm (data not shown). We coupled this "heat bleaching" with modifications of a protocol using tannic acid (Polishchuk *et al.*, 2004) so as to avoid its possible deleterious effects on paracellular permeability and electrical resistance (Paladino *et al.*, 2006; see *Discussion*). By incompletely understood mechanism(s), the cell-impermeant fixative tannic acid blocks dynamic events at the cell surface to which it is added. In our revised protocol, after 4 h at 40°C, polarized MDCK cells were placed for 20 min at 10°C in medium that contained 0.5% tannic acid added selectively to the basolateral compartment. Cells were then returned to 37°C for 15 min with continued exposure to tannic acid in the basolateral medium, at which time there was no effect on transepithelial electrical resistance (TER) and [^{14}C]inulin flux, although increased, remained $<$0.06% (Supplementary Figure 1 and *Discussion*). The inulin flux in our untreated cells was always below 0.03%, much lower than that reported by Paladino and coworkers (0.25%; Paladino *et al.*, 2006). Following 15 min exposure to tannic acid, Naked2 fluorescence appeared at the lower lateral corner (Figure 3B); there was sixfold increased intensity at the base of the cell compared with the subapical region by quantifying the average pixel fluorescent intensity in three *Z*-axis planes from the tight junctions to the base of the cell (1:2.2:6.1; Figure 3B). Under steady state conditions (i.e., returning the cells to 37°C for 2 h in the absence of tannic acid; Figure 3C), Naked2 was found along the entire length of the lateral membrane (1:1.2:1.9). Tannic acid did not affect the basolateral distribution of CD147 (an integral membrane protein) or p120 (a membrane-associated protein; Supplementary Figure 2B). Thus, using two different experimental approaches (live cell microscopy and short exposure to tannic acid in stably transfected, fully polarized MDCK cells), we present evidence that Naked2-associated vesicles are delivered to the lower portion of the lateral plasma membrane in contrast to LDLR and VSV-G, which are delivered to a Sec6/8-containing exocyst complex beneath tight junctions (Kreitzer *et al.*, 2003; Polishchuk *et al.*, 2004).

μ1B-independent Trafficking of Naked2-associated Vesicles to the Basolateral Surface of Polarized LLC-PK1 and MDCK Cells

Two general basolateral sorting motifs have been identified within the cytoplasmic domain of transported proteins. These consist of tyrosine (NPxY and Yxxϕ) and dileucine (D/ExxxL[L/I] and DxxLL) consensus motifs. Cargo selection often is based on interactions between these sorting signals and specific domains on adaptors, although an increasing number of exceptions have been identified (Devonald *et al.*, 2003; Duffield *et al.*, 2004; Folsch, 2005). TGFα contains a dileucine repeat but no tyrosine residues. Naked2 contains two Yxxϕ motifs (Y152EVV and Y247LDL) that are potential recognition sites for μ1B, a subunit of the epithelial-specific heterotetrameric AP-1B complex. We considered that Naked2 might interact with the AP-1 complex; however, transient transfection of Naked2 cDNAs expressing individual tyrosine mutants (Y152A and Y247A) into MDCK cells did not alter their basolateral localization (data not shown). In addition, as described below, Naked2 fragment 1-265 that contains both Yxxϕ motifs did not interact directly with any of the components of the adaptin complex tested by yeast two-hybrid analysis (Figure 4E).

The μ1B subunit of AP-1B is not expressed in LLC-PK1 cells. It has been shown that basolateral cargo like LDLR and transferrin receptor are mis-sorted apically in LLC-PK1 cells and that transfection of μ1B restores basolateral trafficking of both of these receptors (Folsch *et al.*, 1999). This prompted us to examine the localization of Naked2 and TGFα in μ1B-deficient LLC-PK1 cells. Endogenous Naked2 was detected in LLC-PK1 cells, as well as Caco-2 cells, a human colorectal cancer cell line. Both TGFα (Figure 4A) and Naked2 (data not shown) were found at the basolateral membrane of polarized LLC-PK1 cells that had been transfected individually and in combination with epitope-tagged Naked2 and TGFα cDNAs (Figure 4A). Moreover, we transiently transfected Halo-tagged Naked2 cDNA into MDCK cells stably expressing LDLR-EGFP and observed no overlap of LDLR-containing vesicles with Naked2-associated vesicles (Figure 4B), further supporting our contention that trafficking of Naked2-associated vesicles is independent of μ1B.

Studies were then directed toward understanding the relationship between Naked2 and conventional exocytic adaptor protein machinery. We used 10-40% iodoxinal gradient centrifugation to fractionate MDCK cells stably expressing wild-type Naked2-GFP (see *Materials and Methods*). Three Naked2-enriched fractions (3-9, 16, and 18-19) were identified visually by GFP fluorescence and biochemically by Western blotting (Figure 4C, top panel). The broad first fraction contained cell surface (syntaxin 4A, E-cadherin), Golgi (GRASP55, Golgin 97), and ER (calreticulin) proteins, which were de-enriched in the latter two fractions (data not shown). Our confidence in the validity of this Naked2 fractionation scheme is strengthened by finding 1) comigration of Dishevelled1, a protein known to interact with Naked2 (Rousset *et al.*, 2001) and 2) increased levels of TGFα by RIA in the Naked2-enriched fractions (Figure 4C, bottom panel). We observed that antibodies that recognize the β1 and β2 subunit of AP-1 and AP-2, α-adaptin, γ-adaptin, and μ1A comigrated with Naked2-enriched fractions. Adaptin μ1B, μ4, and the heavy chain of clathrin did not comigrate with Naked2 (Figure 4C).

To assess whether the AP-1 and AP-2 complexes interacted directly with Naked2, we performed coimmunofluorescent staining. Endogenous β1/2 adaptins did not colocalize with Naked2 (Figure 4D), nor did γ adaptin, a subunit of both AP-1A and AP-1B complexes. Antibodies useful for immunofluorescent detection of μ1A and μ1B adaptins were not available. We previously reported that Naked2-associated vesicles do not colocalize with fluorescently tagged EGF and transferrin (Li *et al.*, 2004). In addition to these endocytic cargoes, Naked2-GFP did not colocalize with Rab7a, Rab8, Rab11A, Rab11B, myosin Va, b, c, EEA1, α-adaptin, clathrin heavy chain, mCherry-clathrin light chain, or DsRed2-tagged μ2 in paraformaldehyde-fixed cells (data not shown). Naked2-GFP also did not colocalize with Golgi and ER markers (Golgin97, TGN38, GM130, p58, TR-ceramide, or TR-brefeldin A; data not shown).

To examine direct interactions between Naked2 and adaptor proteins, we used Naked2 residues 1-173 and residues 1-265 (data not shown) in yeast two-hybrid analysis with components of the adaptor protein machinery generously provided by J. Bonifacino (Janvier *et al.*, 2003). We observed no direct interactions between Naked2 and components of AP-1, AP-2, AP-3, and AP-4 under adenine minus (data not shown) or less stringent histidine minus growth conditions (Figure 4E). We also considered whether Naked2 might bind to a γ/σ1 dimer of AP-1 in that the HIV protein NEF is myristoylated and acts as a connector by binding both to a cargo CD4 and a γ/σ1 dimer of AP-1 (Rose *et al.*, 2005).

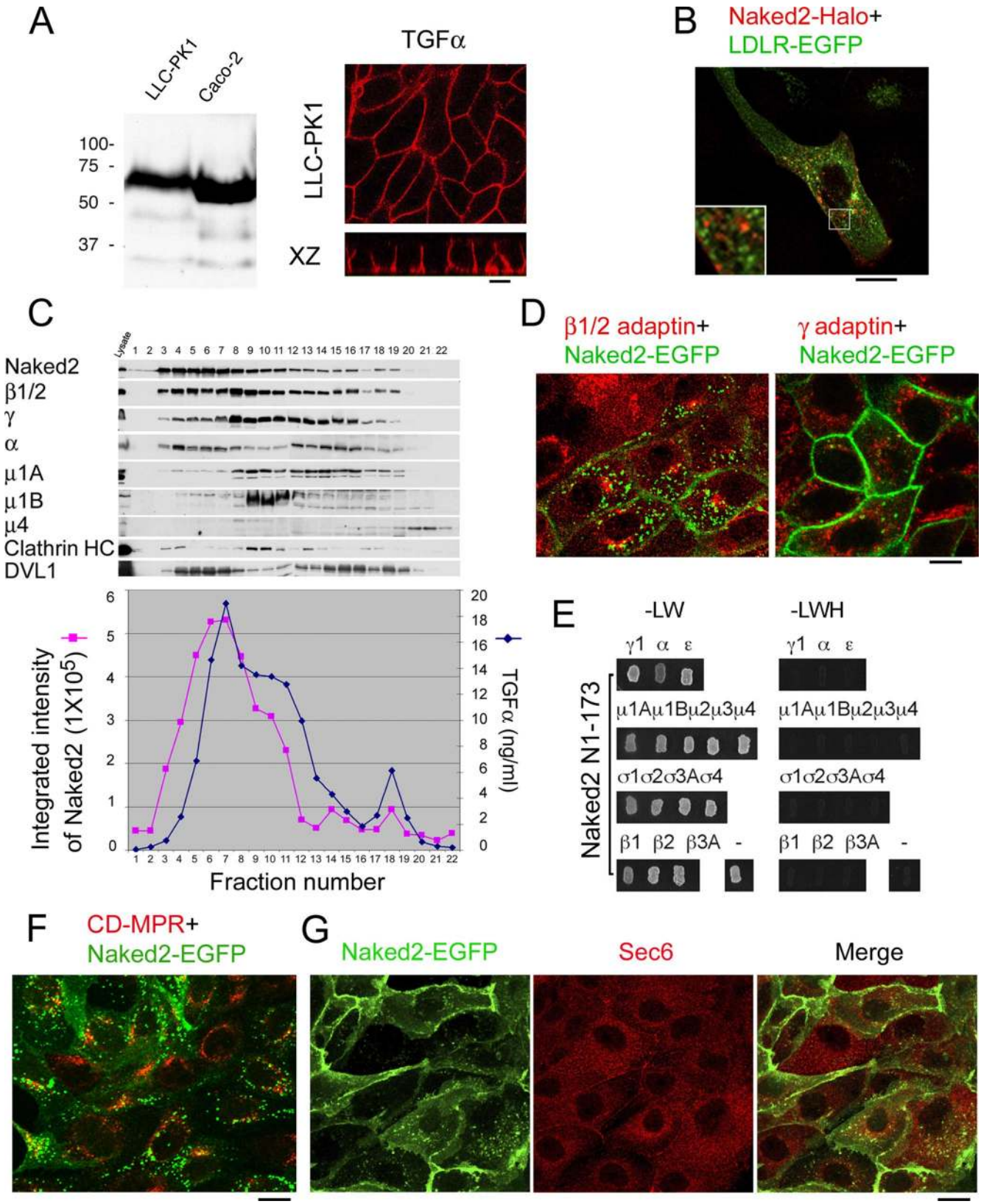

Figure 4. Basolateral delivery of Naked2-associated vesicles does not require μ1B. (A) Endogenous Naked2 was detected by Western blotting of whole cell lysates from these LLC-PK1 cells and Caco-2 cells (a human colon cancer cell line) using R44, a previously described rabbit polyclonal antibody to human Naked2 (Li *et al.*, 2004). HA-tagged TGFα was stably transfected into LLC-PK1 cells. TGFα staining decorates the basolateral compartment of these μ1B-deficient LLC-PK1 cells. (B) Transiently transfected Halo-tagged Naked2 did not colocalize with LDL receptor (LDLR) in MDCK cells that had been stably transfected with LDLR-EGFP. (C) Top, Western blotting of Naked2,

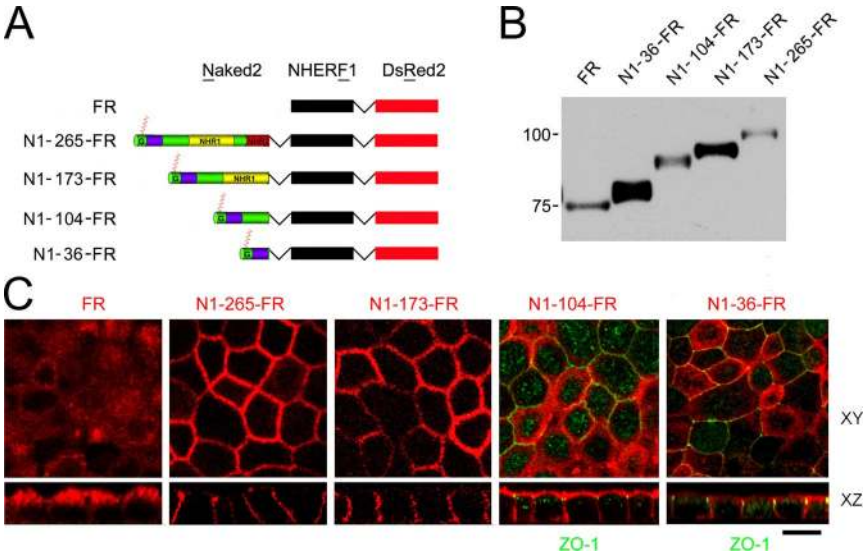

Figure 5. Mapping of Naked2 basolateral targeting domain. (A) Fragments of human Naked2 were fused to human Na^+/H^+ exchanger regulatory factor (NHERF)-1 and dsRed2. These chimeras were transfected stably into MDCK cells. (B) Relative expression of these chimeras by Western blotting. (C) *XY* and *XZ* images of polarized MDCK cells expressing different Naked2 and NHERF-1 chimeras. *XY* images of polarized MDCK cells were obtained at the apex of the cells near the tight junctions (using ZO-1, green, as shown in panels 4 and 5). FR (NHERF-1 fused to dsRed2) showed diffuse staining in the apical cytoplasm of polarized MDCK cells; Naked2 residues 1-265 fused with FR (N1-265-FR) redirected FR to the basolateral plasma membrane like wild-type Naked2. Naked2 residues 1-173 fused with FR (N1-173-FR) also decorated the basolateral plasma membrane. Fusion of N-terminal 1-104 amino acids of Naked2 to FR (N1-104-FR) exhibited strong staining at the apical and basolateral plasma membrane. Naked2 residues 1-36 fused with FR (N1-36-FR) exhibited predominant staining of the apical compartment (cytoplasm and plasma membrane) with weaker staining along the basolateral plasma membrane. Bar, 10 μm.

Naked2, however, did not interact with a $\gamma/\sigma 1$ dimer (data not shown). GGA1, 2, and 3 compose a new family of monomeric adaptors that recognize an acidic amino acid cluster-dileucine motif within the cytoplasmic tails of cargoes (Bonifacino and Traub, 2003; Nakayama and Wakatsuki, 2003). For example, mannose-6-phosphate receptor (CD-MPR) is sorted to endosomes by GGA adaptors (Puertollano *et al.*, 2001); Naked2, however, did not colocalize with CD-MPR in MDCK cells (Figure 4F). Finally, Naked2 did not colocalize with Sec6, part of the exocyst complex that cooperates with the AP-1B complex for basolateral delivery of cargo (Figure 4G).

Collectively, these data provide strong evidence that μ1B adaptin is not required for trafficking of Naked2-associated, TGFα-containing exocytic vesicles to the basolateral membrane of polarized epithelial cells. It appears that LDLR and TGFα utilize a different set of exocytic vesicles for their basolateral transport. There are no direct interactions between Naked2 and AP-1, AP-2, AP-3, and AP-4 by yeast two- or three-hybrid analysis and coimmunostaining. We cannot exclude that adaptors disassemble from vesicles before Naked2 binds TGFα because Naked2 does not colocalize with *trans*-Golgi markers and only recognizes Golgi-processed forms of TGFα (Li *et al.*, 2004). Future studies are designed to address this possibility.

Figure 4 (cont). Dishevelled (DVL1), and endogenous adaptor proteins from fractions isolated from 10 to 40% iodoxinal gradient centrifugation from MDCK cells stably overexpressing Naked2-EGFP and TGFα. Bottom, levels of TGFα by RIA in the different fractions correspond to those enriched for Naked2 by Western blotting. (D) Lack of colocalization of $\beta 1/2$ adaptin and γ adaptin with Naked2 GFP fluorescence. Antibody to β adaptin (10A) recognizes both $\beta 1$ and 2 adaptin. mAb 100.3 is specific for γ adaptin. (E) Yeast two-hybrid analysis between Naked2 N1-173 and different AP subunits under histidine minus growth conditions. This Naked2 fragment did not interact directly with AP-1-4 components. Naked2-EGFP did not colocalize with CD-MPR (F), which is sorted by GGA (Puertollano *et al.*, 2001) or Sec6 (G). Bars, 10 μm.

N-terminus of Naked2 Contains Basolateral Sorting Information

To identify domains that direct Naked2 to the basolateral membrane of polarized MDCK cells, we fused different regions of Naked2 N-terminus fused to human DsRed2-tagged NHERF-1 (FR; Figure 5A) and stably transfected them into MDCK cells. NHERF-1 is a PDZ-containing 358-amino acid protein that is localized to the apical cytoplasm of polarized epithelial cells; it acts as an adaptor protein to assist the apical trafficking of ion transporters, G-protein–coupled receptors and more than 11 other proteins (Reczek *et al.*, 1997; Morales *et al.*, 2004; Shenolikar *et al.*, 2004). Figure 5B displays the intensity and molecular sizes of these chimeras immunoblotted with anti-DsRed2 polyclonal antibody in stably expressing MDCK cells.

As expected, FR fluorescence was observed in the apical cytoplasm (Figure 5C). However, when the N-terminal 265 residues of Naked2 (extending through NHR2) were fused to FR, fluorescence was redistributed from the apical compartment to the basolateral plasma membrane (Figure 5C). There was a similar staining pattern when the Naked2 fragment was shortened to NHR1 (terminating at residue 173) and fused to FR (Figure 5C); however, when the N-terminal 104 residues of Naked2 were fused with FR, there was a loss of basolateral selectivity with the appearance of apical and basolateral membrane fluorescence (Figure 5C). Both apical and basolateral fluorescence were also observed when Naked2 N1-36 was fused with FR. Thus, Naked2 residues 1-173 are necessary and sufficient for basolateral targeting. These findings (that Naked2 residues 1-173 direct the chimera only basolaterally, whereas apical and basolateral fluorescence was observed with residues 1-104) suggest to us that the NHR1 domain (residues 107-173) may contain sufficient information for basolateral trafficking of Naked2. However, when residues 37-104 were deleted within the context of full-length Naked2, there was a loss of basolateral selectivity (Figure 6, B and C) with the appearance of apical as well as basolateral staining, indicating that residues 37-104 are also needed for basolateral targeting of Naked2.

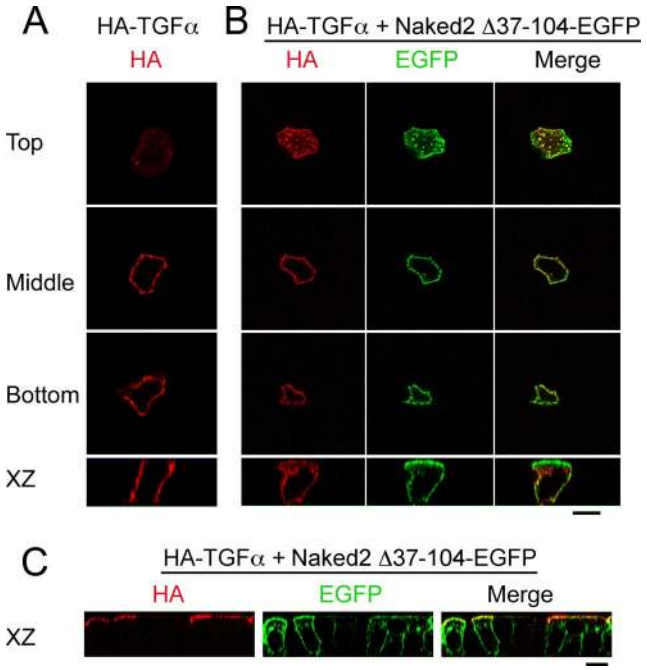

Figure 6. Loss of basolateral selectivity for Naked2 and TGFα with deletion of Naked2 residues 37-104. (A) Normal basolateral membrane localization of HA-tagged TGFα (red) in transiently transfected, polarized MDCK cells. (B) TGFα redistributed apically and partially colocalized with Naked2 Δ37-104-EGFP when MDCK cells were transiently cotransfected with Naked2 Δ37-104-EGFP mutant and HA-tagged TGFα. (C) TGFα was detected at the apical cell surface when HA antibody was added at 4°C to the apical compartment of nonpermeabilized live cells stably cotransfected with HA ectodomain–tagged TGFα and Naked2 Δ37-104-EGFP mutant cDNA constructs. Naked2 fluorescence colocalized with TGFα immunoreactivity at the apical surface. Bars, 10 μm.

It remains formally possible that Naked2 may be directed to the basolateral surface of polarized epithelial cells by TGFα rather than vice versa. To consider this possibility, we examined localization of HA-tagged TGFα in Naked2 Δ37-104-EGFP–expressing MDCK cells. As expected, when N-terminally HA-tagged TGFα alone was transiently transfected into MDCK cells, it localized to the basolateral cell surface (Figure 6A). However, when it was transiently cotransfected with Naked2 Δ37-104-EGFP (Figure 6B), TGFα colocalized with Naked2 in cytoplasmic vesicles and at the apical and basolateral plasma membrane. To confirm this apical mislocalization of TGFα, we performed live cell immunofluorescent staining for TGFα and selectively added hemagglutinin (HA) antibody at 4°C to nonpermeabilized MDCK cells stably transfected with ectodomain HA-TGFα and Naked2 Δ37-104-EGFP cDNA constructs. HA staining selectively decorated the apical surface (Figure 6C). In a separate experiment under identical conditions except that HA antibody was added to the basolateral compartment, HA staining selectively decorated the basolateral membrane (data not shown). These results provide further evidence that Naked2 regulates TGFα cell surface delivery and argue against TGFα directing Naked2 to the cell surface.

Knockdown of Naked2 Results in Increased Cytosolic TGFα Immunoreactivity

We previously identified endogenous Naked2 expression in HaCat cells (Li *et al.*, 2004), a human adult skin–derived spontaneously immortalized keratinocyte cell line. We stably transfected HA-tagged TGFα into HaCat cells; this clone was designated HaCat23. Retroviral-mediated delivery of a human Naked2 29-mer shRNA (shNaked2) resulted in decreased Naked2 protein levels in puromycin-resistant pools of HaCat23 compared with vector-infected, puromycin-resistant pools and parental HaCat23 cells (Figure 7A). Of note, there was a significant accumulation of cytosolic TGFα immunoreactivity in cells treated with Naked2 shRNA (Figure 7B, top panel); the fluorescent intensity was quantified using reconstructed 3D images of 10 fields from confocal micrographs of whole cells (Figure 7B, bottom panel). Western blot of immunoprecipitated TGFα showed a dramatic reduction in the 16-kDa cell surface isoform and a corresponding increase in the 36-kDa Golgi-processed isoform of TGFα in Naked2 shRNA knockdown cells (Figure 7C). These results support our earlier contention that G2A Naked2 acts in dominant negative manner (Li *et al.*, 2004).

DISCUSSION

As initially formulated by George Palade, the vesicle transport hypothesis states that the transfer of cargo molecules between organelles of the secretory pathway is mediated by shuttling transport vesicles (Bonifacino and Glick, 2004). Vesicles bud from a "donor" compartment ("vesicle budding") by a process that allows selective incorporation of cargo into the forming vesicle while retaining resident proteins in the donor compartment ("protein sorting"). The vesicles are then targeted to a specific "acceptor" compartment ("vesicle targeting") into which they unload their cargo upon fusion of their limiting membranes ("vesicle fusion"). At the TGN, it is generally thought that an adaptor complex recognizes basolateral sorting motifs in the cytoplasmic tails of cargo. For example, the μ1B subunit of AP-1 recognizes tyrosine-based motifs (Ohno *et al.*, 1995, 1999), whereas the β1 subunit of AP-1 recognizes dileucine motifs (Rapoport *et al.*, 1998). After cargo recognition by an adaptor, clathrin is recruited, the donor membrane is deformed, vesicles pinch off, clathrin disassembles, and the adaptor is thought to fall off. These now naked vesicles somehow make their way to the basolateral cell surface where the concerted action of soluble *N*-ethylmalemide–sensitive factor attachment protein receptor (vesicle [v]- and target [t]-SNAREs, respectively) and tethers results in vesicle fusion with the plasma membrane (Weber *et al.*, 1998). More recent work has found that sorting may occur at the level of the Golgi and recycling endosomes (Gravotta *et al.*, 2007). Thus, both recycling endosomes and the Golgi appear to act as sorting organelles (Muth and Caplan, 2003; Folsch, 2005; Rodriguez-Boulan *et al.*, 2005).

Mechanisms underlying the actual transport of nascent vesicles to the basolateral cell surface are poorly understood. The current understanding of the site of fusion at the basolateral plasma membrane, based on the study of LDLR and VSV-G, is that basolaterally targeted proteins are directed to a Sec6/8 exocyst complex beneath the tight junctions (Kreitzer *et al.*, 2003; Polishchuk *et al.*, 2004). We present evidence that Naked2 associates with a subclass of exocytic vesicles that contain TGFα, but not LDLR, as a cargo. Naked2 contains the necessary information to direct these post-Golgi vesicles to the lower lateral membrane of polarized MDCK cells. These results expand our understanding of mechanisms underlying basolateral transport and indicate that the Sec6/8 exocyst complex is not an obligatory targeting patch for all basolaterally targeted exocytic vesicles.

At the outset, we considered whether Naked2 might be conveyed passively from the TGN to the basolateral surface

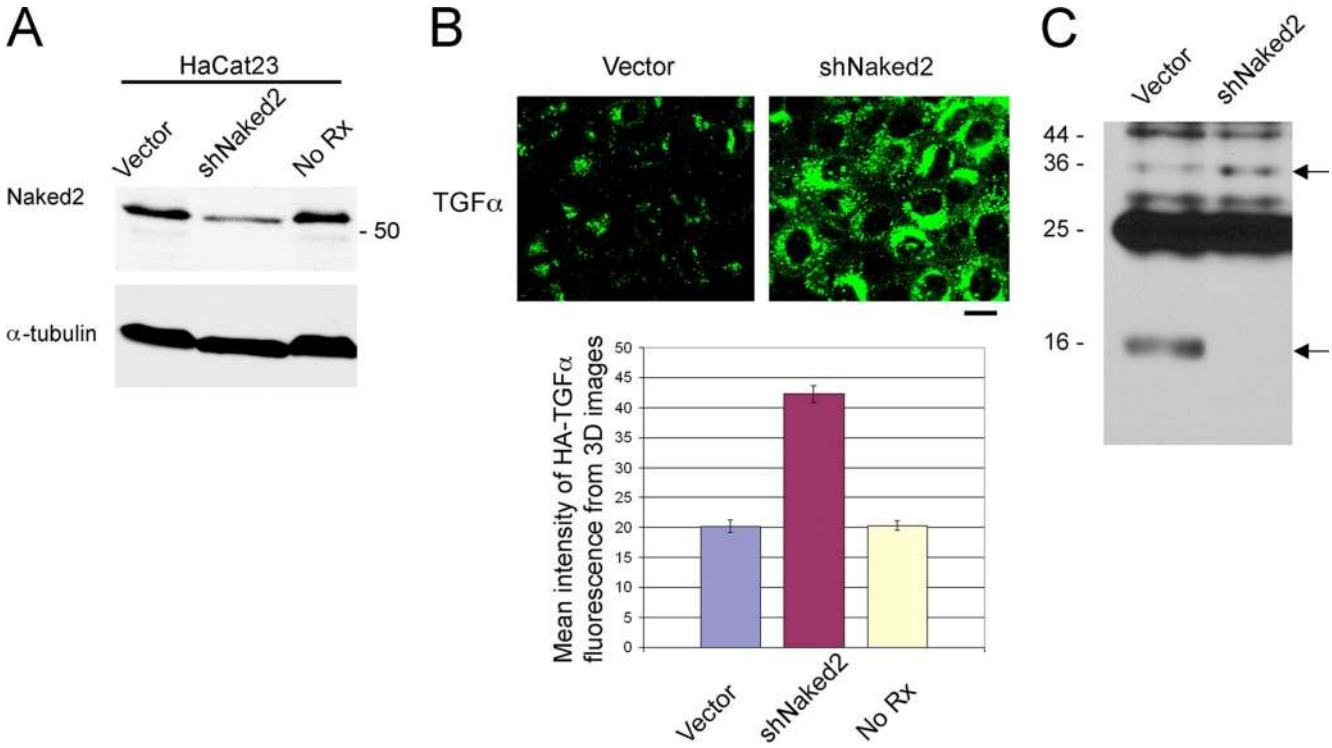

Figure 7. shRNA knockdown of endogenous Naked2 results in increased cytosolic TGFα immunoreactivity with a dramatic reduction in cell surface TGFα. HaCat cells were stably transfected with an HA-tagged–TGFα cDNA; this clone was designated HaCat23. (A) Retroviral-mediated delivery of Naked2 shRNA to HaCat23 cells reduced endogenous Naked2 levels by 60% compared with vector control and parental cells. (B) There was a significant increase of cytosolic TGFα immunoreactivity in Naked2 shRNA-treated cells, as quantified by reconstructed 3D images of 10 fields from confocal micrographs of whole cells; mean intensity ± SD. Student's *t* test, $p < 0.01$. Bar, 10 μm. (C) Western blot of immunoprecipitated TGFα showed a marked reduction in the 16-kDa cell surface isoform and a correspondingly increase of Golgi-processed isoform (36 kDa).

by its interaction with TGFα. Four observations argue against this possibility. First, there are Naked2-associated vesicles that do not contain TGFα in MDCK cells, as assessed by immunohistochemical staining with antibodies directed to both the ectodomain and cytoplasmic tail of TGFα (Li *et al.,* 2004). Second, Naked2-associated vesicles traffick normally to the plasma membrane in MDCK cells expressing a Naked2 mutant in which the TGFα cytoplasmic TTB (residues 300-385) has been deleted (data not shown). Third, Naked2 residues 1-173 that lack TTB completely redirect NHERF-1 from the apical cytoplasm to the basolateral plasma membrane (Figure 5). Finally, deletion of residues 37-104 within full-length Naked2 results in the appearance of TGFα, as well as Naked2, at the apical and basolateral compartment of polarized MDCK cells (Figure 7). Thus, we conclude that Naked2 actively directs TGFα to the basolateral surface of polarized epithelial cells. Naked2 does not appear to act as a conventional chaperone for TGFα because it interacts late in the secretory pathway with the cytoplasmic tail of proTGFα and not the mature protein; nor does Naked2 act merely as a cargo recognition protein because it accompanies its cargo to its destination, transporting TGFα-containing exocytic vesicles to the basolateral membrane where the vesicles dock and fuse in a Naked2 myristoylation-dependent manner (Figure 2; Li *et al.,* 2004).

Naked2 Vesicle Fusion Events

Vesicle-Plasma Membrane Fusion. "Kiss and run," "kiss and coat," and "full fusion" are three types of exocytic vesicle behavior that take place at the plasma membrane in epithelial, chromaffin, and neuronal cells (Schneider, 2001; Sokac and Bement, 2006). By TIR-FM and live cell microscopy, we observed kiss and run and kiss and fusion of Naked2-associated vesicles with the plasma membrane. Such behavior was not observed for myristoylation-deficient G2A mutant–associated vesicles. We do not know whether Naked2 acts independently or collaborates with t-SNAREs (e.g., syntaxin4; Musch *et al.,* 2002), v-SNAREs, and tethers to achieve vesicle fusion. In vitro reconstitution experiments of SNAREs with Naked2 are planned to address this question.

Homotypic Vesicle–Vesicle Fusion. Regulated fusion is mostly carried out between heterotypic membranes (Bonifacino and Glick, 2004; Rodriguez-Boulan *et al.,* 2005). However, in white blood cells, parotid acinar cells, alveolar type II cells, and pancreatic β-cells, homotypic granule–granule fusion occurs intracellularly to form bigger vesicles before exocytic fusion with the plasma membrane (Sutton *et al.,* 1998; Weber *et al.,* 1998; Hu *et al.,* 2003; Pickett and Edwardson, 2006) in what is considered to be a maturation process. Homotypic Naked2 vesicle kiss and run and fusion events were seen frequently by live cell microscopy. The significance of Naked2 vesicle–vesicle fusion is unknown; it may increase the efficiency of exocytosis and/or represent an active state of vesicle communication, maturation, or sorting. It certainly underscores the dynamic nature of these exocytic vesicles. In contrast, G2A Naked2 vesicles exhibited no social behavior, i.e., no vesicle–vesicle or vesicle–plasma membrane fusion events. These results indicate myristoylation is required to

mediate Naked2-associated vesicle fusion events. Future studies will address whether myristoylation of Naked2 is a regulated process like conformational regulation of the ARF1 myristoyl moiety by GTP hydrolysis (Goldberg, 1999).

N-terminus of Naked2 Confers Basolateral Directionality. Little is known about mechanisms underlying directional transport of basolateral vesicles following the TGN to the basolateral plasma membrane, although it is accepted that basolateral vesicles can be passively recruited by special structures such as the exocyst, t-SNARE/syntaxin4 or adhesion molecules (Yeaman *et al.*, 2004). We used different strategies to elucidate an active role for Naked2 in this process. NHERF1 is localized at the apical cytoplasm of polarized epithelial cells and acts as an adaptor protein to assist apical trafficking (Reczek *et al.*, 1997; Morales *et al.*, 2004; Shenolikar *et al.*, 2004). We demonstrated that residues 1-173 of Naked2 were able to completely redirect NHERF-1 from the apical compartment to the basolateral plasma membrane; however, the N-terminal 104 residues of Naked2 (both N1-104 and N1-36 fusion constructs; Figure 5C) were insufficient, suggesting that residues 104-173 may contain all of the information needed for basolateral targeting. However, deletion of residues 37-104 within the context of wild-type Naked2 resulted in loss of basolateral selectivity, with this deletion mutant localizing to both the apical and basolateral plasma membrane. Thus, residues 37-104 are necessary but not sufficient for basolateral directionality. The N-terminal 36 amino acids, together with myristoylation of Naked2, are also not sufficient for basolateral directionality (Figure 5C), although they are necessary for membrane anchoring.

We speculate that the sequence E37EAERRAR within residues 37-51 may form a regulatable hairpin structure to control myristoyl moiety open-closed status like ARFs or to interact with a special basolateral structure. Similar sequences are found within transmembrane protein 132A (TMEM132A), translational initiation factor (IF-2), and cytoskeleton-regulatory proteins (such as plectins and Dishevelled-associated activator of morphogenesis 2), but it is not known how they act. Identification of a basolateral directing domain within Naked2 is a novel finding for an adaptor protein. An immediate question is how Naked2 N37-173 fragment recognizes its targeting track and docking site. E-cadherin and Nectin-2α have been identified to recruit the Sec6/8 exocyst to the lateral membrane and then to act as the active fusion site for LDLR- and VSV-G–containing vesicles (Yeaman *et al.*, 2004). Apparently, the known Naked2 binding proteins, TGFα and Dishevelled, are not important for trafficking, because their binding sites can be removed without affecting Naked2 basolateral targeting. Future studies will be needed to identify the components of the selective docking sites and associated tethers for Naked2-associated vesicles.

Naked2-coated Vesicles Target Initially to the Lower Portion of the Basolateral Surface of MDCK Cells

Basolateral fusion of exocytic vesicles based on tyrosine sorting signals has been reported to take place at the upper portion of the lateral plasma membrane associated with the Sec6/8 exocyst and AP-1B complex (Kreitzer *et al.*, 2003; Polishchuk *et al.*, 2004). LDLR fusion was shown at this site by time-lapse confocal microscopy (Kreitzer *et al.*, 2003), and Shrew-1 and VSV-G fusion was found at this site by tannic acid–blocking experiments (Polishchuk *et al.*, 2004; Jakob *et al.*, 2006). In polarized MDCK cells, the Sec6/8 complex is recruited to (Yeaman *et al.*, 2004) and localized at the apical junctional complex along the lateral membrane (Grindstaff *et al.*, 1998; Lipschutz *et al.*, 2000), which is recognized to be an area of active exocytosis (Kreitzer *et al.*, 2003). We previously reported that Naked2-associated vesicles accumulated asymmetrically at the basolateral corner of MDCK cells stably expressing myristoylation-deficient G2A Naked2. In the present studies, we used two independent strategies to examine the site of delivery of wild-type Naked2-associated vesicles. By live cell microscopy, we show that Naked2-coated vesicles are delivered to the lower portion of the lateral plasma membrane (Figure 2). In addition, we administered tannic acid selectively to the basolateral medium to block dynamic events at the basolateral cell surface. Addition of cell-impermeant tannic acid to the apical or basolateral compartment of polarized MDCK II cells has been used by Lippincott-Schwartz's lab as a tool to study vesicle delivery and transcytosis (Polishchuk *et al.*, 2004). More recently, Paladino *et al.* (2006) used this method to study apical sorting of GPI-anchored proteins in MDCK II cells. These investigators emphasized the importance of using stably transfected cell lines and fully polarized cells when employing tannic acid blockade, and they cautioned that longer term exposure to tannic acid might disrupt tight junctional integrity. These two reports prompted us to examine the temporal effects of tannic acid alone on these two parameters for stably transfected MDCK cells that were maintained on Transwell filters for different periods of time (Supplementary Figure 1). Under our experimental conditions, it appears that tannic acid alone has no significant effects on TER. It does appear that tannic acid increases [^{14}C]inulin flux; however, this did not increase above 0.1% under any condition tested over a 30-min time course (Supplementary Figure 1), which implied that the monolayer integrity of MDCK cells was retained (Apodaca *et al.*, 1995). By only exposing stably transfected, fully polarized MDCK II cells to tannic acid for 15 min (without cycloheximide or trypsin), we feel that we have circumvented problems related to disruption of junctional integrity related to longer term exposure to tannic acid in transiently transfected, partially polarized MDCK II cells. Moreover, our experiments were designed to address direct delivery and not transcytosis of trafficking proteins.

Taken together, these studies identify a number of functions performed by Naked2 to ensure the successful delivery of TGFα to the basolateral surface of polarized epithelial cells. It recognizes post-Golgi TGFα-containing vesicles and directs these vesicles to a basolateral corner of polarized epithelial cells where the vesicles then dock and fuse in a Naked2 myristoylation-dependent manner. Should Naked2 be considered a coat, a chaperone, an adaptor, or a connector? None of these terms seem especially apt. Although it recognizes a cargo, it is not a conventional coat or adaptor because evidence has not been presented that it forms a higher ordered oligomeric structure nor does it disassemble from the vesicle before reaching the acceptor organelle. Presently, we prefer to designate Naked2 a CaRT protein. We predict that additional functionally similar yet structurally distinct CARTs will be identified as the complexity and heterogeneity of basolateral trafficking is increasingly appreciated. Many questions remain. Does Naked2's myristoylation site undergo conformation-dependent sequestration and exposure, perhaps regulated by calcium or GTP? How are Naked2 mRNA and protein regulated? Wild-type Naked2 protein has a half-life of ~30 min, which is much shorter than conventional coat and adaptor proteins. Are there specific proteins at the basolateral corner or on the track to the basolateral corner recognized by Naked2? If so, does this represent the basal equivalent of planar cell polarity in which proteins

assemble asymmetrically at the apical surface? What is the protein and lipid composition of Naked2-associated vesicles? We have identified 389 proteins by LC-MS/MS from biochemically enriched, flow-sorted Naked2-associated vesicles in G2A-Naked2-EGFP–expressing MDCK cells in which the myristoylation-deficient Naked2 vesicles are trapped in the cytoplasm; this includes a number of motors, kinesins, and Rab proteins (Zheng Cao and Robert J. Coffey, unpublished data). It is clear that the detailed study of Naked2 has and will continue to reveal new insights into the intricacies of basolateral trafficking in polarized epithelial cells.

ACKNOWLEDGMENTS

The authors thank James R. Goldenring for reviewing the manuscript and Marilyn Resh (Memorial Sloan Kettering Cancer Center) and Heike Folsch (Northwestern University) for helpful comments. We highly appreciate sharing of reagents from the laboratories of J. Bonifacino, M. S. Robinson, I. Mellman, M. Traub, S. Honing, M. J. Caplan (Yale University School of Medicine), and T. Kirchausen. This work was supported by grants from the National Cancer Institute (CA 46413), the GI Special Program of Research Excellence (CA 95103), and the Mouse Models of Human Cancers Consortium (U01 084239) to R.J.C.

REFERENCES

Apodaca, G., Bomsel, M., Lindstedt, R., Engel, J., Frank, D., Mostov, K. E., and Wiener-Kronish, J. (1995). Characterization of *Pseudomonas aeruginosa*-induced MDCK cell injury: glycosylation-defective host cells are resistant to bacterial killing. Infect. Immun. *63*, 1541–1551.

Bonifacino, J. S., and Glick, B. S. (2004). The mechanisms of vesicle budding and fusion. Cell *116*, 153–166.

Bonifacino, J. S., and Traub, L. M. (2003). Signals for sorting of transmembrane proteins to endosomes and lysosomes. Annu. Rev. Biochem. *72*, 395–447.

Briley, G. P., Hissong, M. A., Chiu, M. L., and Lee, D. C. (1997). The carboxyl-terminal valine residues of proTGF alpha are required for its efficient maturation and intracellular routing. Mol. Biol. Cell *8*, 1619–1631.

Dempsey, P. J., and Coffey, R. J. (1994). Basolateral targeting and efficient consumption of transforming growth factor-alpha when expressed in Madin-Darby canine kidney cells. J. Biol. Chem. *269*, 16878–16889.

Dempsey, P. J., Meise, K. S., and Coffey, R. J. (2003). Basolateral sorting of transforming growth factor-alpha precursor in polarized epithelial cells: characterization of cytoplasmic domain determinants. Exp. Cell Res. *285*, 159–174.

Devonald, M. A., Smith, A. N., Poon, J. P., Ihrke, G., and Karet, F. E. (2003). Non-polarized targeting of AE1 causes autosomal dominant distal renal tubular acidosis. Nat. Genet. *33*, 125–127.

Duffield, A., Folsch, H., Mellman, I., and Caplan, M. J. (2004). Sorting of H, K-ATPase beta-subunit in MDCK and LLC-PK cells is independent of mu 1B adaptin expression. Traffic *5*, 449–461.

Fernandez-Larrea, J., Merlos-Suarez, A., Urena, J. M., Baselga, J., and Arribas, J. (1999). A role for a PDZ protein in the early secretory pathway for the targeting of proTGF-alpha to the cell surface. Mol. Cell *3*, 423–433.

Folsch, H. (2005). The building blocks for basolateral vesicles in polarized epithelial cells. Trends Cell Biol. *15*, 222–228.

Folsch, H., Ohno, H., Bonifacino, J. S., and Mellman, I. (1999). A novel clathrin adaptor complex mediates basolateral targeting in polarized epithelial cells. Cell *99*, 189–198.

Franklin, J. L., Yoshiura, K., Dempsey, P. J., Bogatcheva, G., Jeyakumar, L., Meise, K. S., Pearsall, R. S., Threadgill, D., and Coffey, R. J. (2005). Identification of MAGI-3 as a transforming growth factor-alpha tail binding protein. Exp. Cell Res. *303*, 457–470.

Goldberg, J. (1999). Structural and functional analysis of the ARF1-ARFGAP complex reveals a role for coatomer in GTP hydrolysis. Cell *96*, 893–902.

Gravotta, D., Deora, A., Perret, E., Oyanadel, C., Soza, A., Schreiner, R., Gonzalez, A., and Rodriguez-Boulan, E. (2007). AP1B sorts basolateral proteins in recycling and biosynthetic routes of MDCK cells. Proc. Natl. Acad. Sci. USA *104*, 1564–1569.

Grindstaff, K. K., Yeaman, C., Anandasabapathy, N., Hsu, S. C., Rodriguez-Boulan, E., Scheller, R. H., and Nelson, W. J. (1998). Sec6/8 complex is recruited to cell-cell contacts and specifies transport vesicle delivery to the basal-lateral membrane in epithelial cells. Cell *93*, 731–740.

Harris, R. C., Chung, E., and Coffey, R. J. (2003). EGF receptor ligands. Exp. Cell Res. *284*, 2–13.

Hirschberg, K., Miller, C. M., Ellenberg, J., Presley, J. F., Siggia, E. D., Phair, R. D., and Lippincott-Schwartz, J. (1998). Kinetic analysis of secretory protein traffic and characterization of golgi to plasma membrane transport intermediates in living cells. J. Cell Biol. *143*, 1485–1503.

Hu, C., Ahmed, M., Melia, T. J., Sollner, T. H., Mayer, T., and Rothman, J. E. (2003). Fusion of cells by flipped SNAREs. Science *300*, 1745–1749.

Jakob, V., Schreiner, A., Tikkanen, R., and Starzinski-Powitz, A. (2006). Targeting of transmembrane protein Shrew-1 to adherens junctions is controlled by cytoplasmic sorting motifs. Mol. Biol. Cell. *17*, 3397–3408.

Janvier, K., Kato, Y., Boehm, M., Rose, J. R., Martina, J. A., Kim, B. Y., Venkatesan, S., and Bonifacino, J. S. (2003). Recognition of dileucine-based sorting signals from HIV-1 Nef and LIMP-II by the AP-1 gamma-sigma1 and AP-3 delta-sigma3 hemicomplexes. J. Cell Biol. *163*, 1281–1290.

Kreitzer, G., Schmoranzer, J., Low, S. H., Li, X., Gan, Y., Weimbs, T., Simon, S. M., and Rodriguez-Boulan, E. (2003). Three-dimensional analysis of post-Golgi carrier exocytosis in epithelial cells. Nat. Cell Biol. *5*, 126–136.

Kuo, A., Zhong, C., Lane, W. S., and Derynck, R. (2000). Transmembrane transforming growth factor-alpha tethers to the PDZ domain-containing, Golgi membrane-associated protein p59/GRASP55. EMBO J. *19*, 6427–6439.

Li, C., Franklin, J. L., Graves-Deal, R., Jerome, W. G., Cao, Z., and Coffey, R. J. (2004). Myristoylated Naked2 escorts transforming growth factor alpha to the basolateral plasma membrane of polarized epithelial cells. Proc. Natl. Acad. Sci. USA *101*, 5571–5576.

Li, Q., Ishikawa, T. O., Miyoshi, H., Oshima, M., and Taketo, M. M. (2005). A targeted mutation of Nkd1 impairs mouse spermatogenesis. J. Biol. Chem. *280*, 2831–2839.

Lipschutz, J. H., Guo, W., O'Brien, L. E., Nguyen, Y. H., Novick, P., and Mostov, K. E. (2000). Exocyst is involved in cystogenesis and tubulogenesis and acts by modulating synthesis and delivery of basolateral plasma membrane and secretory proteins. Mol. Biol. Cell *11*, 4259–4275.

Morales, F. C., Takahashi, Y., Kreimann, E. L., and Georgescu, M. M. (2004). Ezrin-radixin-moesin (ERM)-binding phosphoprotein 50 organizes ERM proteins at the apical membrane of polarized epithelia. Proc. Natl. Acad. Sci. USA *101*, 17705–17710.

Musch, A., Cohen, D., Yeaman, C., Nelson, W. J., Rodriguez-Boulan, E., and Brennwald, P. J. (2002). Mammalian homolog of *Drosophila* tumor suppressor lethal (2) giant larvae interacts with basolateral exocytic machinery in Madin-Darby canine kidney cells. Mol. Biol. Cell *13*, 158–168.

Muth, T. R., and Caplan, M. J. (2003). Transport protein trafficking in polarized cells. Annu. Rev. Cell Dev. Biol. *19*, 333–366.

Nakayama, K., and Wakatsuki, S. (2003). The structure and function of GGAs, the traffic controllers at the TGN sorting crossroads. Cell Struct. Funct. *28*, 431–442.

Ohno, H., Stewart, J., Fournier, M. C., Bosshart, H., Rhee, I., Miyatake, S., Saito, T., Gallusser, A., Kirchhausen, T., and Bonifacino, J. S. (1995). Interaction of tyrosine-based sorting signals with clathrin-associated proteins. Science *269*, 1872–1875.

Ohno, H., Tomemori, T., Nakatsu, F., Okazaki, Y., Aguilar, R. C., Foelsch, H., Mellman, I., Saito, T., Shirasawa, T., and Bonifacino, J. S. (1999). Mu1B, a novel adaptor medium chain expressed in polarized epithelial cells. FEBS Lett. *449*, 215–220.

Paladino, S., Pocard, T., Catino, M. A., and Zurzolo, C. (2006). GPI-anchored proteins are directly targeted to the apical surface in fully polarized MDCK cells. J. Cell Biol. *172*, 1023–1034.

Pickett, J. A., and Edwardson, J. M. (2006). Compound exocytosis: mechanisms and functional significance. Traffic *7*, 109–116.

Polishchuk, R., Di Pentima, A., and Lippincott-Schwartz, J. (2004). Delivery of raft-associated, GPI-anchored proteins to the apical surface of polarized MDCK cells by a transcytotic pathway. Nat. Cell Biol. *6*, 297–307.

Puertollano, R., Aguilar, R. C., Gorshkova, I., Crouch, R. J., and Bonifacino, J. S. (2001). Sorting of mannose 6-phosphate receptors mediated by the GGAs. Science *292*, 1712–1716.

Rapoport, I., Chen, Y. C., Cupers, P., Shoelson, S. E., and Kirchhausen, T. (1998). Dileucine-based sorting signals bind to the beta chain of AP-1 at a site distinct and regulated differently from the tyrosine-based motif-binding site. EMBO J. *17*, 2148–2155.

Reczek, D., Berryman, M., and Bretscher, A. (1997). Identification of EBP50, a PDZ-containing phosphoprotein that associates with members of the ezrin-radixin-moesin family. J. Cell Biol. *139*, 169–179.

Rodriguez-Boulan, E., Kreitze, G., and Musch, A. (2005). Organization of vesicular trafficking in epithelia. Nat. Rev. Mol. Cell Biol. *6*, 233–247.

Rose, J. J., Janvier, K., Chandrasekhar, S., Sekaly, R. P., Bonifacino, J. S., and Venkatesan, S. (2005). CD4 down-regulation by HIV-1 and simian immunodeficiency virus (SIV) Nef proteins involves both internalization and intracellular retention mechanisms. J. Biol. Chem. *280*, 7413–7426.

Rousset, R., Mack, J. A., Wharton, K. A., Jr., Axelrod, J. D., Cadigan, K. M., Fish, M. P., Nusse, R., and Scott, M. P. (2001). Naked cuticle targets dishevelled to antagonize Wnt signal transduction. Genes Dev. *15*, 658–671.

Rousset, R., Wharton, K. A., Jr., Zimmermann, G., and Scott, M. P. (2002). Zinc-dependent interaction between dishevelled and the *Drosophila* Wnt antagonist naked cuticle. J. Biol. Chem. *277*, 49019–49026.

Schneider, S. W. (2001). Kiss and run mechanism in exocytosis. J. Membr. Biol. *181*, 67–76.

Shenolikar, S., Voltz, J. W., Cunningham, R., and Weinman, E. J. (2004). Regulation of ion transport by the NHERF family of PDZ proteins. Physiology (Bethesda) *19*, 362–369.

Sokac, A. M., and Bement, W. M. (2006). Kiss-and-coat and compartment mixing: coupling exocytosis to signal generation and local actin assembly. Mol. Biol. Cell *17*, 1495–1502.

Sunnarborg, S. W. *et al.* (2002). Tumor necrosis factor-alpha converting enzyme (TACE) regulates epidermal growth factor receptor ligand availability. J. Biol. Chem. *277*, 12838–12845.

Sutton, R. B., Fasshauer, D., Jahn, R., and Brunger, A. T. (1998). Crystal structure of a SNARE complex involved in synaptic exocytosis at 2.4 A resolution. Nature *395*, 347–353.

Weber, T., Zemelman, B. V., McNew, J. A., Westermann, B., Gmachl, M., Parlati, F., Sollner, T. H., and Rothman, J. E. (1998). SNAREpins: minimal machinery for membrane fusion. Cell *92*, 759–772.

Wharton, K. (2003). Runnin' with the Dvl: proteins that associate with Dsh/Dvl and their significance to Wnt signal transduction. Dev. Biol. *253*, 1–17.

Yan, D., Wallingford, J. B., Sun, T. Q., Nelson, A. M., Sakanaka, C., Reinhard, C., Harland, R. M., Fantl, W. J., and Williams, L. T. (2001). Cell autonomous regulation of multiple Dishevelled-dependent pathways by mammalian Nkd. Proc. Natl. Acad. Sci. USA *98*, 3802–3807.

Yeaman, C., Grindstaff, K. K., and Nelson, W. J. (2004). Mechanism of recruiting Sec6/8 (exocyst) complex to the apical junctional complex during polarization of epithelial cells. J. Cell Sci. *117*, 559–570.